

Search for CP violation in $\tau \rightarrow \pi\pi^0\nu_\tau$ decay.(CLEO Collaboration)
(April 3, 2000)**Abstract**

We search for CP non-conservation in the decays of τ leptons produced via e^+e^- annihilation at $\sqrt{s} \sim 10.6$ GeV. The method uses correlated decays of pairs of τ leptons, each decaying to the $\pi\pi^0\nu_\tau$ final state. The search is done within the framework of a model with a scalar boson exchange. In an analysis of a data sample corresponding to 12.2 million produced τ pairs collected with the CLEO detector, we find no evidence of violation of CP symmetry. We obtain a limit on the imaginary part of the coupling constant parameterizing the relative contribution of diagrams that would lead to CP violation to be $-0.046 < \Im(\Lambda) < 0.022$ at 90% C.L. This result provides a restriction on CP non-conservation in the tau lepton decays. As a cross check, we study the decay angular distribution and perform a model-independent search for a CP violation effect of a scalar exchange in single $\tau \rightarrow \pi\pi^0\nu_\tau$ decays. The limit on the imaginary part of the τ scalar coupling is $-0.033 < \Im(\Lambda) < 0.089$ at 90% C.L.

P. Avery,¹ C. Prescott,¹ A. I. Rubiera,¹ H. Stoeck,¹ J. Yelton,¹ G. Brandenburg,²
 A. Ershov,² D. Y.-J. Kim,² R. Wilson,² T. Bergfeld,³ B. I. Eisenstein,³ J. Ernst,³
 G. E. Gladding,³ G. D. Gollin,³ R. M. Hans,³ E. Johnson,³ I. Karliner,³ M. A. Marsh,³
 C. Plager,³ C. Sedlack,³ M. Selen,³ J. J. Thaler,³ J. Williams,³ K. W. Edwards,⁴
 A. J. Sadoff,⁵ R. Ammar,⁶ A. Bean,⁶ D. Besson,⁶ X. Zhao,⁶ S. Anderson,⁷ V. V. Frolov,⁷
 Y. Kubota,⁷ S. J. Lee,⁷ J. J. O'Neill,⁷ R. Poling,⁷ A. Smith,⁷ C. J. Stepaniak,⁷ J. Urheim,⁷
 S. Ahmed,⁸ M. S. Alam,⁸ S. B. Athar,⁸ L. Jian,⁸ L. Ling,⁸ M. Saleem,⁸ S. Timm,⁸
 F. Wappler,⁸ A. Anastassov,⁹ E. Eckhart,⁹ K. K. Gan,⁹ C. Gwon,⁹ T. Hart,⁹
 K. Honscheid,⁹ D. Hufnagel,⁹ H. Kagan,⁹ R. Kass,⁹ T. K. Pedlar,⁹ J. B. Thayer,⁹
 E. von Toerne,⁹ M. M. Zoeller,⁹ S. J. Richichi,¹⁰ H. Severini,¹⁰ P. Skubic,¹⁰ A. Undrus,¹⁰
 V. Savinov,¹¹ S. Chen,¹² J. Fast,¹² J. W. Hinson,¹² J. Lee,¹² D. H. Miller,¹² E. I. Shibata,¹²
 I. P. J. Shipsey,¹² V. Pavlunin,¹² D. Cronin-Hennessy,¹³ A.L. Lyon,¹³ E. H. Thorndike,¹³
 T. E. Coan,¹⁴ V. Fadeyev,¹⁴ Y. S. Gao,¹⁴ Y. Maravin,¹⁴ I. Narsky,¹⁴ R. Stroynowski,¹⁴
 J. Ye,¹⁴ T. Wlodek,¹⁴ M. Artuso,¹⁵ C. Boulahouache,¹⁵ K. Bukin,¹⁵ E. Dambasuren,¹⁵
 G. Majumder,¹⁵ R. Mountain,¹⁵ S. Schuh,¹⁵ T. Skwarnicki,¹⁵ S. Stone,¹⁵ J.C. Wang,¹⁵
 A. Wolf,¹⁵ J. Wu,¹⁵ S. Kopp,¹⁶ M. Kostin,¹⁶ A. H. Mahmood,¹⁷ S. E. Csorna,¹⁸ I. Danko,¹⁸
 K. W. McLean,¹⁸ Z. Xu,¹⁸ R. Godang,¹⁹ G. Bonvicini,²⁰ D. Cinabro,²⁰ M. Dubrovin,²⁰
 S. McGee,²⁰ G. J. Zhou,²⁰ A. Bornheim,²¹ E. Lipeles,²¹ S. P. Pappas,²¹ A. Shapiro,²¹
 W. M. Sun,²¹ A. J. Weinstein,²¹ D. E. Jaffe,²² R. Mahapatra,²² G. Masek,²² H. P. Paar,²²
 D. M. Asner,²³ A. Eppich,²³ T. S. Hill,²³ R. J. Morrison,²³ R. A. Briere,²⁴ G. P. Chen,²⁴
 T. Ferguson,²⁴ H. Vogel,²⁴ A. Gritsan,²⁵ J. P. Alexander,²⁶ R. Baker,²⁶ C. Bebek,²⁶
 B. E. Berger,²⁶ K. Berkelman,²⁶ F. Blanc,²⁶ V. Boisvert,²⁶ D. G. Cassel,²⁶ P. S. Drell,²⁶
 J. E. Duboscq,²⁶ K. M. Ecklund,²⁶ R. Ehrlich,²⁶ P. Gaidarev,²⁶ R. S. Galik,²⁶ L. Gibbons,²⁶
 B. Gittelman,²⁶ S. W. Gray,²⁶ D. L. Hartill,²⁶ B. K. Heltsley,²⁶ P. I. Hopman,²⁶ L. Hsu,²⁶
 C. D. Jones,²⁶ J. Kandaswamy,²⁶ D. L. Kreinick,²⁶ M. Lohner,²⁶ A. Magerkurth,²⁶
 T. O. Meyer,²⁶ N. B. Mistry,²⁶ E. Nordberg,²⁶ M. Palmer,²⁶ J. R. Patterson,²⁶
 D. Peterson,²⁶ D. Riley,²⁶ A. Romano,²⁶ H. Schwarthoff,²⁶ J. G. Thayer,²⁶ D. Uner,²⁶
 B. Valant-Spaight,²⁶ G. Viehhauser,²⁶ and A. Warburton²⁶

¹University of Florida, Gainesville, Florida 32611

²Harvard University, Cambridge, Massachusetts 02138

³University of Illinois, Urbana-Champaign, Illinois 61801

⁴Carleton University, Ottawa, Ontario, Canada K1S 5B6

and the Institute of Particle Physics, Canada

⁵Ithaca College, Ithaca, New York 14850

⁶University of Kansas, Lawrence, Kansas 66045

⁷University of Minnesota, Minneapolis, Minnesota 55455

⁸State University of New York at Albany, Albany, New York 12222

⁹Ohio State University, Columbus, Ohio 43210

¹⁰University of Oklahoma, Norman, Oklahoma 73019

¹¹University of Pittsburgh, Pittsburgh, Pennsylvania 15260

¹²Purdue University, West Lafayette, Indiana 47907

¹³University of Rochester, Rochester, New York 14627

¹⁴Southern Methodist University, Dallas, Texas 75275

¹⁵Syracuse University, Syracuse, New York 13244

¹⁶University of Texas, Austin, Texas 78712

- ¹⁷University of Texas - Pan American, Edinburg, Texas 78539
- ¹⁸Vanderbilt University, Nashville, Tennessee 37235
- ¹⁹Virginia Polytechnic Institute and State University, Blacksburg, Virginia 24061
- ²⁰Wayne State University, Detroit, Michigan 48202
- ²¹California Institute of Technology, Pasadena, California 91125
- ²²University of California, San Diego, La Jolla, California 92093
- ²³University of California, Santa Barbara, California 93106
- ²⁴Carnegie Mellon University, Pittsburgh, Pennsylvania 15213
- ²⁵University of Colorado, Boulder, Colorado 80309-0390
- ²⁶Cornell University, Ithaca, New York 14853

I. INTRODUCTION

Violation of the combined symmetry of charge conjugation and parity (CP) has been of long-standing interest as a possible source of the matter-antimatter asymmetry [1] in the Universe. Efforts to search for CP-violating effects have concentrated so far on the hadronic sector: CP violation in strange meson decay has been the subject of intensive investigation since its first observation in 1964 [2]. Recent studies of hadronic [3] as well as semileptonic [4–6] kaon decays provide precision measurements of the CP violation parameters. Searches for corresponding asymmetries in B meson decays are the focus of several large ongoing experiments [7,8]. Recent indications of possible neutrino oscillations [9] make it important to re-examine the question of CP non-conservation in the leptonic sector. Such violation is forbidden in the Standard Model but appears as a consequence of various extensions [10]. Models predicting lepton flavor violation often also predict CP violation in lepton decays [11,12]. Among theoretically best-known are the multi-Higgs-doublet models (MHDM) [13–15]. In this paper, we study CP violation in τ decay, in the context of a model with scalar boson exchange [16,17]. The results of the search are general but are easiest to interpret for a specific choice of MHDM. Precision studies of muon decay parameters [18,19] show no indication for a CP violation in such decay. Previous attempts to study this question in tau decays [20,21] provide only weak restrictions on the CP violation parameters.

The search is carried out using data collected with the CLEO detector operating at the Cornell Electron Storage Ring (CESR), where τ leptons are produced in pairs $e^+e^- \rightarrow \tau^+\tau^-$. Specifically, we study events in which both τ 's decay to the $\pi\pi^0\nu_\tau$ final state. In such events, interference between the Standard Model process involving W -boson exchange and a non-Standard Model one involving scalar boson exchange can give rise to observable CP-violating terms. For each event we compute a quantity for which a non-zero expectation value would constitute evidence for CP violation.

This article is organized as follows. A general description of CP violation in the leptonic sector is given in Section II. An observable used to search for CP violation is described in Section III. The data analysis and its results are in Sections IV and V. A model-independent search for scalar-mediated τ decays is described in Section VI. Derivations of elements of the probability density distribution for a pair of τ leptons each decaying into $\pi\pi^0\nu_\tau$ final states and theoretical calculations used in optimizing the choice of the CP-sensitive variable are given in appendices.

II. CP VIOLATION IN LEPTON DECAY

CP violation generates a difference between the partial decay width for a process ($i \rightarrow f$) and the corresponding width for its CP-conjugated process ($i^{CP} \rightarrow f^{CP}$). Any kinematical observable ξ associated with a decay can be described as a sum of CP-even and CP-odd components:

$$\xi = \xi_{even} + \xi_{odd}. \quad (1)$$

The average value of this observable is equal to an integral of ξ over all available phase space multiplied by the probability density, P , for the decay. This probability density also can be, in general, decomposed into CP-even and CP-odd components:

$$P = P_{even} + P_{odd}. \quad (2)$$

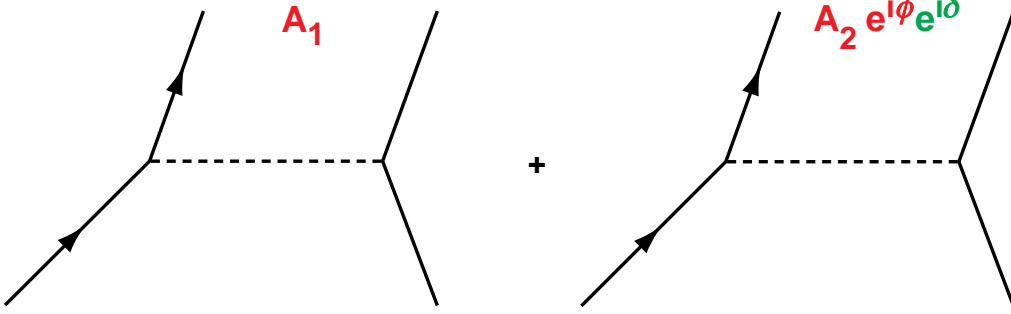


FIG. 1. Interference between two amplitudes with CP-even and CP-odd relative phases δ and ϕ .

The average value of ξ is:

$$\begin{aligned} \langle \xi \rangle_{i \rightarrow f} &= \int (\xi_{even} + \xi_{odd}) P dLips = \int (\xi_{even} + \xi_{odd}) (P_{even} + P_{odd}) dLips \\ &= \int \xi_{even} P_{even} dLips + \int \xi_{odd} P_{odd} dLips. \end{aligned} \quad (3)$$

Under CP conjugation P_{odd} changes sign and the average value of the observable ξ for the decay of the CP-conjugated state is:

$$\begin{aligned} \langle \xi \rangle_{i^{CP} \rightarrow f^{CP}} &= \int (\xi_{even} + \xi_{odd}) P^{CP} dLips = \int (\xi_{even} + \xi_{odd}) (P_{even} - P_{odd}) dLips \\ &= \int \xi_{even} P_{even} dLips - \int \xi_{odd} P_{odd} dLips. \end{aligned} \quad (4)$$

If P_{odd} is not equal to zero, then $\langle \xi \rangle_{i \rightarrow f} \neq \langle \xi \rangle_{i^{CP} \rightarrow f^{CP}}$ and CP is violated.

A lepton decay process described by two amplitudes illustrated in Fig. 1 may have CP-even and CP-odd phases δ and ϕ relative to each other. The probability density for such a process is given by:

$$\begin{aligned} |\mathcal{A}|^2 &= (A_1 + A_2 e^{i\phi} e^{i\delta})(A_1 + A_2 e^{-i\phi} e^{-i\delta}) \\ &= A_1^2 + A_2^2 + 2A_1 A_2 \cos \phi \cos \delta - \underline{2A_1 A_2 \sin \phi \sin \delta}. \end{aligned} \quad (5)$$

The last, underlined, term is CP-odd since the phase ϕ changes sign under CP conjugation. In this example the CP-odd term is not equal to zero if A_1 , A_2 , $\sin \phi$, and $\sin \delta$ are not equal to zero. A_1 and A_2 denote the amplitudes and for physical processes they must be different from zero. Thus CP-odd term is not equal to zero if the factors $e^{i\phi}$ and $e^{i\delta}$ differ from zero and are complex. We discuss in the following section a theoretical model that satisfies these requirements.

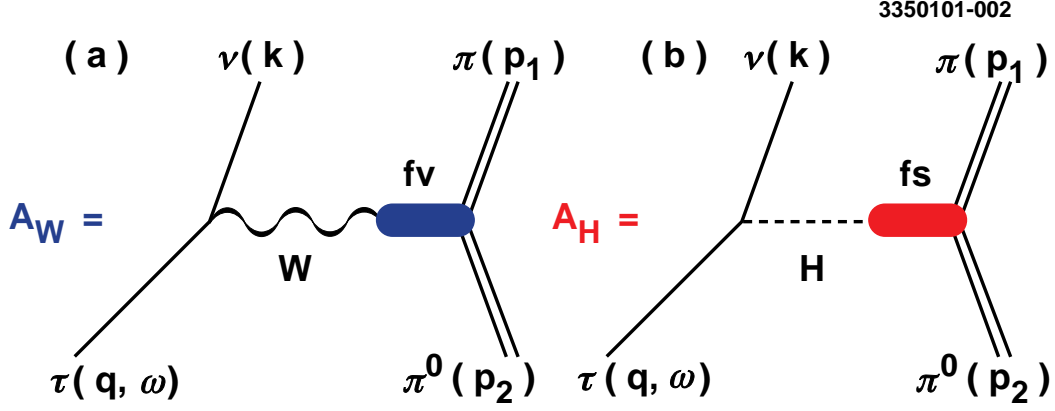


FIG. 2. Amplitude for (a) standard W exchange, (b) scalar exchange.

A. CP violation in τ decays

A possible scenario for CP violation in τ lepton decays is described [13] by the interference of the Standard Model decay amplitude mediated by the W boson (amplitude A_W) with the amplitude mediated by the charged Higgs boson in the multi-Higgs-doublet model¹ (amplitude A_H). These amplitudes play the roles of A_1 and A_2 of the previous section. In this scenario, the charged Higgs couples to quarks and leptons with complex coupling constants and, thus, there can be a weak complex (CP violating) phase ($\sin \phi \neq 0$). The usual choice for the CP-even phase δ is a strong phase [23] which arises due to the QCD final state interactions between quarks. In the following, we consider only τ decays into hadronic final states and a neutrino. The τ decay process is described by a sum of two amplitudes: Standard Model W exchange illustrated in Fig. 2(a) and a scalar exchange illustrated in Fig. 2(b).

To maximize our sensitivity to possible CP-violating effects, we optimize our experimental procedures in the context of a specific model that allows us to calculate the matrix element and the probability density function for τ decay [24]. We have elected to study τ decay into the $\pi^\pm \pi^0 \nu_\tau$ final state due to its large branching fraction, its distinctive experimental signature and its relatively simple hadronic dynamics. However, the procedure is general and can be applied to a number of other final states.

The Standard Model amplitude for τ decay into two pions via the W exchange can be written as:

$$A_W \sim \bar{u}(\nu) \gamma_\mu (1 - \gamma_5) u(\tau) \underbrace{f_v}_{|f_v| e^{i\delta_v}} Q^\mu, \quad (6)$$

where the hadronic current is parameterized by the relative momentum between the charged and neutral pions $Q^\mu = p_1^\mu - p_2^\mu$ multiplied by the vector form factor, f_v , described by ρ Breit-Wigner

¹The three-Higgs-doublet model (3HDM) is the least complicated extension of the Standard Model allowing for CP violation in τ decays [22].

shape:

$$f_v = \frac{-m^2}{s - m^2 + im\Gamma(s)}, \quad (7)$$

where s is a squared invariant mass of two pions, m_π is a pion mass, and m and $\Gamma(s)$ are the mass and the momentum-dependent width of the resonance, respectively. The latter is defined as:

$$\Gamma(s) = \begin{cases} \frac{m}{\sqrt{s}} \left(\frac{s-4m_\pi^2}{m^2-4m_\pi^2} \right)^{3/2} & \text{if } s > (2m_\pi)^2 \\ 0 & \text{elsewhere.} \end{cases} \quad (8)$$

Here, we neglect the contribution from the ρ' resonance [25].

The amplitude for the τ decay into $\pi^\pm \pi^0$ via a charged Higgs boson in the 3HDM model can be written as [13]:

$$A_H \sim \bar{u}(\nu)(1 - \gamma_5)u(\tau) \underbrace{\frac{m_\tau}{m_{Higgs}^2} [m_u Z^* X - m_d Z^* Y]}_{\Lambda} \underbrace{f_s}_{|f_s|e^{i\delta_s}} M, \quad (9)$$

where m_τ , m_{Higgs} , m_u , and m_d are the masses of the tau lepton, charged Higgs, u quark and d quark, respectively.

X , Y , and Z are the ratios of the complex Higgs couplings to u , d quarks and leptons relative to the Standard Model weak couplings. The overall Higgs coupling to the $\pi\pi^0$ system is denoted by Λ :

$$\Lambda = \frac{m_\tau}{m_{Higgs}^2} [m_u Z^* X - m_d Z^* Y]. \quad (10)$$

Because Λ is complex, the CP-odd phase, ϕ , comes from the imaginary part of the coupling constant:

$$\Lambda = \Re(\Lambda) + i\Im(\Lambda) = |\Lambda|(\cos \phi + i \sin \phi). \quad (11)$$

We parameterize the hadronic current as a product of a dimensional quantity, $M = 1 \text{ GeV}/c^2$ providing overall normalization, and a scalar form factor $f_s \equiv |f_s|e^{i\delta_s}$. Here δ_s is a complex strong phase associated with scalar exchange.

The choice of f_s is not unambiguous. We study three cases: one with $f_s = 1$, the second with f_s described by the $a_0(980)$ Breit-Wigner shape and the third with f_s described by $a_0(1450)$ Breit-Wigner shape (see Eq. 7) with a width given by:

$$\Gamma(s) = \begin{cases} \frac{m}{\sqrt{s}} \left(\frac{s-4m_\pi^2}{m^2-4m_\pi^2} \right)^{1/2} & \text{if } s > (2m_\pi)^2 \\ 0 & \text{elsewhere.} \end{cases} \quad (12)$$

The matrix element for the $\tau \rightarrow \pi\pi^0\nu_\tau$ decay is given by the sum of the W and Higgs exchange processes:

$$M(\tau^- \rightarrow \pi^- \pi^0 \nu_\tau) = A_W + A_H, \quad (13)$$

and is given by a sum of terms defined by equations 6 and 9:

$$M(\tau^- \rightarrow \pi^- \pi^0 \nu_\tau) \sim \bar{u}(k)\gamma_\mu(1 - \gamma_5)u(q, s)|f_v|e^{i\delta_v}Q^\mu + \Lambda \bar{u}(k)(1 + \gamma_5)u(q, s)|f_s|e^{i\delta_s}M, \quad (14)$$

where q is the 4-momentum vector of the τ , s is the polarization of the τ and k is the 4-momentum vector of the neutrino.

After calculations detailed in Appendix A the squared matrix element takes the form:

$$|\mathcal{M}|_{\tau^\pm \rightarrow \pi^\pm \pi^0 \nu}^2 \sim G + s^\mu \omega_\mu, \quad (15)$$

where the spin-averaged component of the total width is:

$$\begin{aligned} G = & 2|f_v|^2 [2(qQ)(kQ) - (kq)Q^2] + 2|\Lambda|^2 |f_s|^2 (qk) \\ & + 4\Re(\Lambda) |f_v| |f_s| \cos \delta M_\tau(Qk) - \underline{4\Im(\Lambda^+) |f_v| |f_s| \sin \delta M_\tau(Qk)}, \end{aligned} \quad (16)$$

and the product of the tau polarization s^μ and the polarimeter vector ω_μ describing the spin-dependent component of the decay width is:

$$\begin{aligned} \omega_\mu = & \{ \mp 2|f_v|^2 M_\tau (2Q_\mu(kQ) - k_\mu Q^2) \pm 2|\Lambda|^2 |f_s|^2 M_\tau k_\mu \\ & \mp 4\Re(\Lambda) |f_v| |f_s| \cos \delta (Q_\mu(kq) - k_\mu(qQ)) \\ & \pm \underline{4\Im(\Lambda^+) |f_v| |f_s| \sin \delta (Q_\mu(kq) - k_\mu(qQ))} \\ & + 4\Re(\Lambda) |f_v| |f_s| \sin \delta e_{\mu\alpha\beta\gamma} q^\alpha Q^\beta k^\gamma + \underline{4\Im(\Lambda^+) |f_v| |f_s| \cos \delta e_{\mu\alpha\beta\gamma} q^\alpha Q^\beta k^\gamma} \}. \end{aligned} \quad (17)$$

Here the difference between the strong phases for the vector and scalar exchanges is denoted as $\delta \equiv \delta_v - \delta_s$. The parameter Λ^+ is defined to be equal to Λ for τ^- and equal to its complex conjugate, Λ^* , for τ^+ . Underlined terms are CP-odd.

B. CP violation in correlated decays of τ pairs

For a single τ decay we do not know the polarization vector and consequently can not construct the spin-dependent term. However, the situation is different for decays of pairs of τ 's produced in e^+e^- annihilations, where the parent virtual photon introduces correlations of the τ^+ and τ^- spins. In the following we denote the momenta of the particles deriving from τ^+ with an additional bar symbol in order to distinguish them from the momenta of the τ^- decay products. The probability density for the reaction $e^+e^- \rightarrow \tau^+\tau^-$ can be written as:

$$P_{\tau^+\tau^- \rightarrow \pi^-\pi^0 \nu \pi^+\pi^0 \bar{\nu}} = G \times [(p\bar{q})^2 + (\bar{p}\bar{q})^2 + m_\tau(\bar{p}p)] \times \bar{G} + \omega_\mu \tilde{C}^{\mu\nu} \bar{\omega}_\nu, \quad (18)$$

where p , \bar{p} , q , and \bar{q} are momenta of electron, positron, τ^- , and τ^+ , respectively. The polarimeter vectors of the τ^- and τ^+ are contracted through the spin-correlation matrix $\tilde{C}^{\alpha\beta}$ (see Appendix B for detailed calculations).

The probability density for τ -pair production and the subsequent decay of each τ into the $\pi\pi^0$ final state consists of all CP-even and odd terms from the single τ decay contracted either through the spin-averaged production of the τ pair $(p\bar{q})^2 + (\bar{p}\bar{q})^2 + m_\tau(\bar{p}p)$ or through the spin-correlation matrix $\tilde{C}^{\mu\nu}$ with CP-even and odd terms of the other τ decay (Eq. 15). Due to the spin correlation, these contracted terms are no longer proportional to the spins of the individual τ leptons and, therefore, they do not vanish after integration over all Lorentz-invariant phase space.

To design an optimal method for searching for CP violation, we separate the CP-even and CP-odd terms in the τ production and decay probability density (Eq. 18). We refer to the sum of all CP-even and CP-odd terms as P_{even} and P_{odd} , respectively:

$$P = P_{even} + P_{odd}. \quad (19)$$

Formulae for P_{even} and P_{odd} are given in Appendix C. Both the CP-even and CP-odd parts of the cross section are functions of the kinematical quantities that characterize the τ^+ and τ^- decays.

III. EXPERIMENTAL METHOD

A. Optimal variable

A common method used in searches for CP violation is to define a CP-odd observable ξ , such as, e.g., a triple product of independent vectors, and then average its distribution over the data set. An average of ξ different from zero indicates the presence of a CP-odd component, $P_{odd}(\Lambda)$, of the probability density which, in general, depends on scalar coupling Λ . The choice of the CP-odd observable is not unique. One can always add any CP-odd term to any selected CP-odd observable to obtain another CP-odd observable. Different observables have, in general, different sensitivity to CP violation. To maximize the sensitivity of our search we construct an optimal variable, ξ , with the smallest associated statistical error. Such a variable was proposed by Atwood and Soni [26] and by Gunion and Grzadkowski [27] for other searches. The derivation of ξ is described in detail in Appendix D. The variable is equal to the ratio of the CP-odd and CP-even parts of the total cross section assuming that the absolute value of the coupling Λ is unity:

$$\xi = \frac{P_{odd}(1)}{P_{even}}. \quad (20)$$

The average value of ξ is:

$$\langle \xi \rangle = \int \frac{P_{odd}(1)}{P_{even}} (P_{even} + P_{odd}(\Lambda)) dLips = \int \frac{P_{odd}(1)P_{odd}(\Lambda)}{P_{even}} dLips. \quad (21)$$

Since P_{odd} is proportional to the imaginary part of Λ , we can express it as:

$$P_{odd}(\Lambda) = \Im(\Lambda)P_{odd}(1), \quad (22)$$

and

$$\langle \xi \rangle = \Im(\Lambda) \int \frac{P_{odd}(1)^2}{P_{even}} dLips. \quad (23)$$

The integral in Eq. 23 is always larger than or equal to zero, and equality occurs only if the odd part of the cross section vanishes. Therefore, we expect that the average value of ξ will be proportional to the imaginary part of the Higgs coupling constant and will be positive if $\Im(\Lambda) > 0$ and negative if $\Im(\Lambda) < 0$. Monte Carlo simulation of the ξ distributions for the three choices of scalar form factors and no CP violation² are shown in Fig. 3(a). The same distributions for the CP violating case $\Im(\Lambda) = 1$ are shown in Fig. 3(b). The structure in these distributions is due to the resonant structure in the vector and scalar form factors.

²We use a modified version of the TAUOLA τ decay simulation package [28] to generate Monte Carlo samples corresponding to different values of the complex coupling Λ .

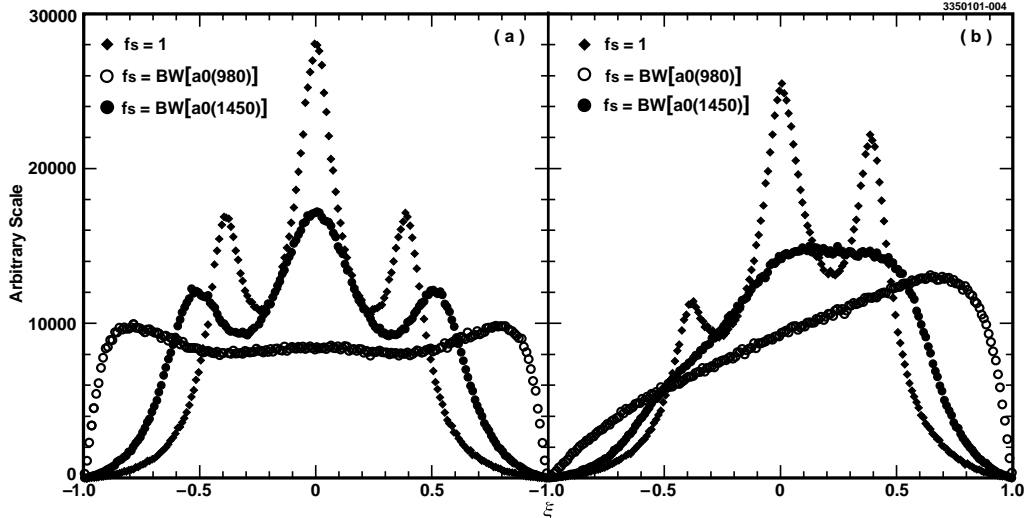


FIG. 3. Optimal observable, ξ , for (a) Monte Carlo with no CP violation and (b) Monte Carlo with a maximal CP violation $\Im(\Lambda) = 1$.

B. Experimental issues

To calculate a value of ξ as described in Section III A, we need to know the directions of the outgoing neutrinos, or equivalently the directions of the τ 's. In cases where both τ 's decay to semi-hadronic final states with two missing neutrinos we can use energy and momentum constraints to determine these directions with a two-fold ambiguity [29]. We assume that in the e^+e^- annihilation the two taus are produced back to back and we ignore the effects of initial state radiation. We cannot distinguish the correct solution from the incorrect one. We check that the wrong solution does not introduce any asymmetry (discussed below) and we sum the ξ distributions obtained from the two solutions. Finally, we calculate the mean value of the summed ξ distribution to search for any evidence of asymmetry.

To assess the possible bias in computed ξ values, we use the KORALB/TAUOLA Monte Carlo to calculate the mean value of the CP-odd observable for the correct and incorrect solutions separately, as well as for the sum of the two. Within errors, we observe no artificial asymmetry in the ξ distribution for the false solution in the Standard Model Monte Carlo sample. However, in the sample with CP violation, the asymmetry obtained using just the false solution is significantly different from that obtained using the correct solution. The Monte Carlo procedure used to calibrate this effect is described in Section V.

IV. DATA ANALYSIS

A. Data and Monte Carlo Samples

The data used in this analysis were collected at the Cornell Electron Storage Ring (CESR) at or near the energy of the $\Upsilon(4S)$. The data correspond to a total integrated luminosity of 13.3 fb^{-1} and contain 12.2 million $\tau^+\tau^-$ pairs. Versions of the CLEO detector employed here are described

in Refs. [30] and [31]. From this data sample, we select events consistent with $e^+e^- \rightarrow \tau^+\tau^-$ interactions where each τ decays into the $\pi\pi^0\nu_\tau$ final state. We refer to such events as ρ - ρ events since this final state is dominated by production and decay of the $\rho(770)$ resonance. The event selection criteria are summarized in Section IV B.

To estimate backgrounds we analyze large samples of Monte Carlo events following the same procedures that are applied to the actual CLEO data. The physics of τ -pair production and decay is modeled by the KORALB/TAUOLA event generator [28], while the detector response is handled with a GEANT-based [32] simulation of the CLEO detectors. For backgrounds coming from τ decays other than $\tau \rightarrow \pi\pi^0\nu_\tau$, we analyze a Monte Carlo sample containing 37.2 million $\tau^+\tau^-$ events in which all combinations of τ^+ and τ^- decay modes are present, except for our signal ρ - ρ process.

Non- τ background processes include annihilation into multihadronic final states, namely $e^+e^- \rightarrow q\bar{q}$ ($q = u, d, s, c$ quarks) and $e^+e^- \rightarrow \Upsilon(4S) \rightarrow B\bar{B}$, as well as production of hadronic final states due to two-photon interactions. Backgrounds from multihadronic physics are estimated using Monte Carlo samples which are slightly larger than the CLEO data and contain 42.6 million $q\bar{q}$ and 17.3 million $B\bar{B}$ events, respectively. The background due to two-photon processes is estimated from Monte Carlo simulation of 37,556 $2\gamma \rightarrow \tau^+\tau^-$ events, using the formalism of Budnev *et al.* [33]. All non-tau backgrounds are found to be negligible (see Section IV.C).

To study the potential bias of the mean value of the observable ξ (Eq. 20) that can be introduced by data selection, we use Monte Carlo samples generated with and without CP violation. The “Standard Model” sample (no CP violation) consists of 2.4 million ρ - ρ events. The equivalent integrated luminosity of this Monte Carlo samples corresponds to four times that of the CLEO data set. Each sample of the CP-violating Monte Carlo contains 1.5 million events.

B. Event Selection.

Tau leptons are produced in pairs in e^+e^- collisions. The event selection follows mostly the procedure developed originally for the study of the $\tau \rightarrow \rho\nu_\tau$ decays [34]. At CESR beam energies, the decay products of the τ^+ and τ^- are well separated in the CLEO detector. We require an event to contain exactly two reconstructed charged tracks, separated in angle by at least 90° . The net charge of the event must be equal to zero. Both tracks must be consistent with originating from e^+e^- interaction region to reject events arising from beam-gas interactions or from cosmic muons passing through the detector. Each track must have a momentum smaller than $0.85 E_{beam}$ to minimize background from Bhabha scattering and muon pair production. The momenta of all charged tracks are corrected for dE/dx energy loss in the beam pipe and tracking system. No attempt is made to distinguish π^\pm from charged leptons or K^\pm mesons: all charged particles are assumed to be pions.

Clusters of energy deposition in the calorimeter are considered as candidates for photons from π^0 decay if they are observed in the central part of the detector ($|\cos\theta| < 0.707$, where θ is the angle between the positron beam axis and the photon direction), are not matched to a charged track, and have energy greater than 30 MeV. A cluster must have a transverse energy profile consistent with expectations for a photon, and it must be at least 30 cm away from the nearest track projection. We select events with only four photon candidates. Pairs of photons with a reconstructed invariant mass $M_{\gamma\gamma}$ between -4 and $+3$ standard deviations ($\sigma_{\gamma\gamma}$) of the π^0 mass are considered to be π^0 candidates. The π^0 invariant mass resolution, $\sigma_{\gamma\gamma}$, varies from 4 to 7 MeV/ c^2 , depending on the

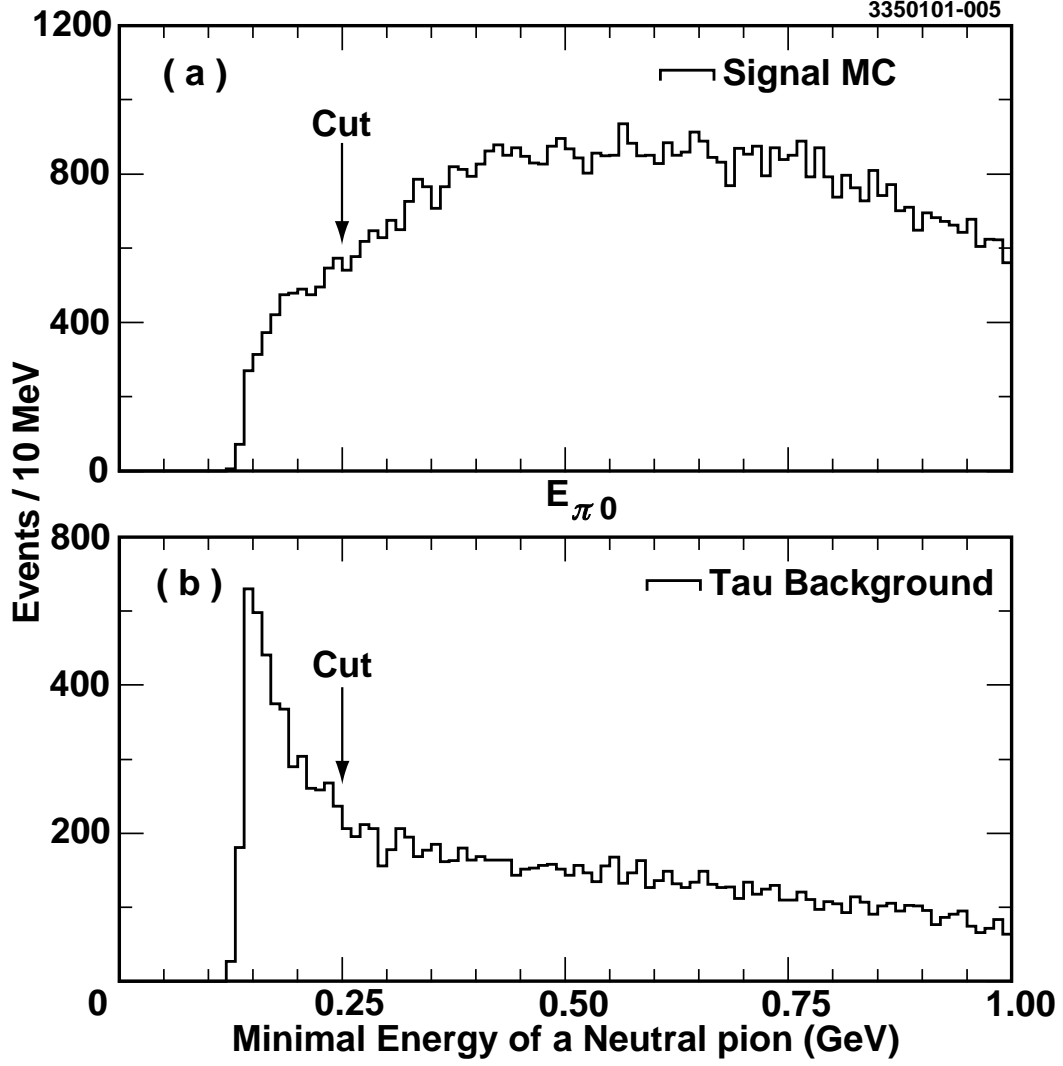


FIG. 4. Energy of the neutral pions: (a) signal Monte Carlo, (b) tau background.

π^0 energy and decay angle. To reject events with spurious π^0 candidates resulting from random combinations of low energy clusters, the π^0 energy is required to be greater than 250 MeV (see Fig. 4). Each π^0 candidate is associated with the nearest in angle charged track to form a $\pi\pi^0$ candidate. Monte Carlo studies show that this method of assignment is correct 99% of the time.

The event selection criteria successfully rejects background from high multiplicity multihadronic events ($e^+e^- \rightarrow q\bar{q}$). Background from low-multiplicity two-photon ($e^+e^- \rightarrow e^+e^-\gamma\gamma$) events are rejected by requiring that the missing transverse momentum be larger than 200 MeV/c and that the missing mass of the event to be smaller than 7.5 GeV/ c^2 (see Fig. 5). Overall, data selection efficiency is estimated to be 7.4%. Extensive systematic studies of the background dependence on selection criteria cuts have been done in Ref. [34] and confirmed by the present work.

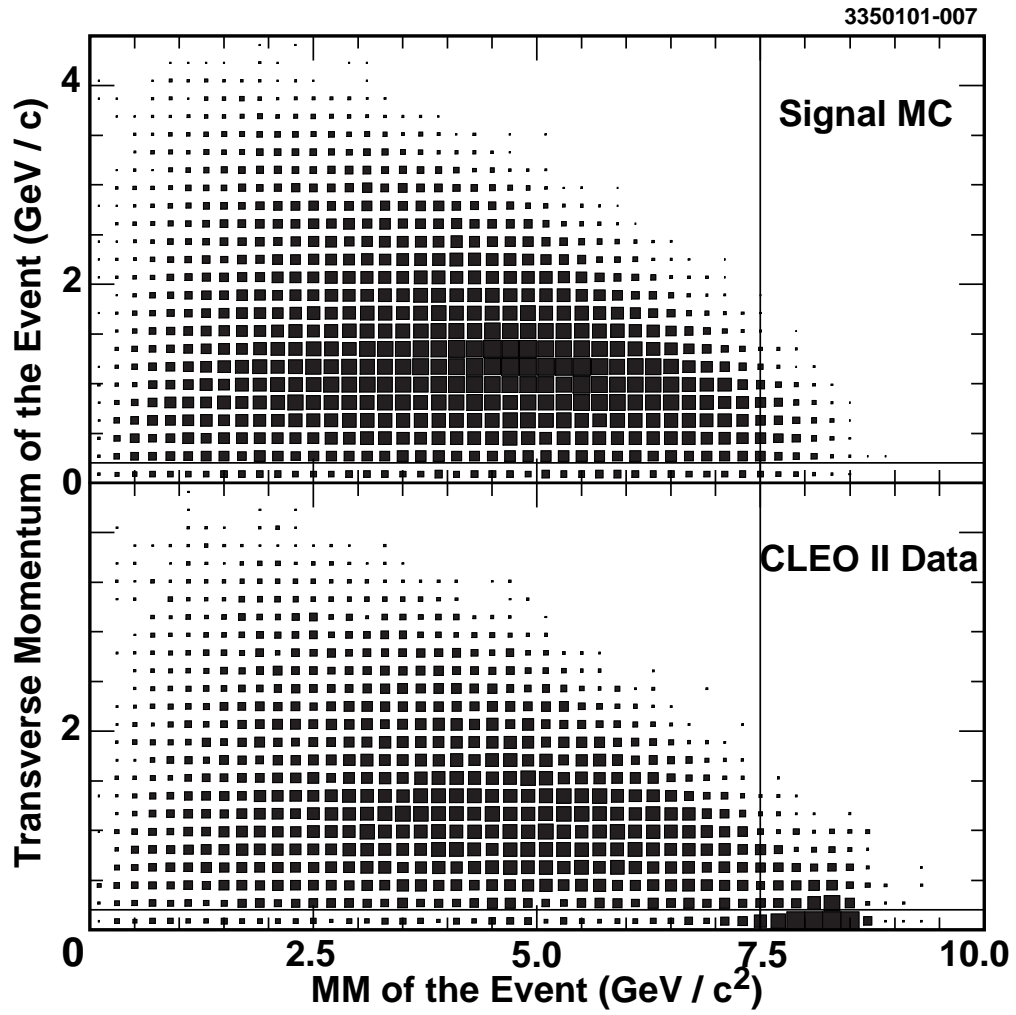


FIG. 5. Transverse momentum and missing mass of the event for the data and signal Monte Carlo. The vertical line indicates the position of the cut.

C. Estimate of the remaining background

After applying the same selection criteria to the Monte Carlo simulation of $e^+e^- \rightarrow q\bar{q}$ and $e^+e^- \rightarrow e^+e^-\gamma\gamma$ processes, we estimated that the remaining background from those sources represents less than 0.1% of the selected data sample. Consequently we ignore this background in our extraction of $\langle \xi \rangle$. We also find no evidence for contribution of cosmic ray or beam-gas interactions in the selected data. The main remaining background is due to the τ -pair events in which one of the τ 's decays into $\rho\nu_\tau$ while the other decays into $\pi 2\pi^0\nu_\tau$ and the photons from one of the π^0 's are not detected. The contamination from this background source is estimated to be 5.2%. The second largest background contribution of 2.1% is due to one of the τ 's decaying into the $K^*\nu_\tau$ final state producing a neutral pion plus a charged kaon which is mistaken for a pion. All other tau decays provide much smaller contributions with the largest being less than 0.7%. The total background contamination from tau decays is estimated to be 9.9%.

V. RESULTS

A. Calibration of the parameterization after applying selection criteria

To relate the observed mean value of the optimal observable, $\langle \xi \rangle$, to the imaginary part of the coupling constant Λ , the $\Im(\Lambda)$ dependence of $\langle \xi \rangle$ must be known. To simplify the notation, in the following we define λ to be the imaginary part of the scalar coupling constant Λ .

The CP-even terms for each single tau decay are either independent of λ or proportional to λ^2 , while CP-odd terms are either linear functions of λ or proportional to λ^3 . Therefore, ξ , which is a product of CP-even and CP-odd terms, must have only odd power terms in λ expansion and to the first order the mean value is proportional to λ with a proportionality coefficient c :

$$\langle \xi \rangle = c \times \lambda. \quad (24)$$

To check this assertion and to calculate the regions of λ where the linear dependence holds we generated 21 event-generator-level Monte Carlo samples (no detector simulation) with different values of λ varying between -1 and 1, and calculated the mean value $\langle \xi \rangle$ for each one. Each sample comprised 10^6 events. For each form of the scalar component, the calculated asymmetry distribution was then fit to a fifth order polynomial (see Fig. 6). Using these distribution we find the ranges of λ for which $\langle \xi \rangle$ is linear in λ . As an additional cross-check of our method, we search for (and find no evidence of) terms proportional to even powers of λ .

Measurement errors can introduce a bias in the ξ distribution (see Eq. 20) as well as change the linearity coefficient c (Eq. 24) due to event selection, reconstruction and resolution. Therefore, this coefficient is calculated after applying selection criteria to events generated with full GEANT-based detector simulation and pattern recognition software. For each choice of the scalar form factor f_s we use five samples of 200,000 signal Monte Carlo events generated with different values of λ in the region where $\langle \xi \rangle$ is linear in λ . For each sample, we calculate the average value of the optimal observable and plot it as a function of λ . For each form of the scalar component, the calculated asymmetry distribution is fit to a straight line to obtain the calibration coefficients. To check that the selection criteria do not create an artificial asymmetry we calculate the mean value of the optimal observable for Standard Model Monte Carlo samples for each choice of the scalar form factor. We list these values along with calculated coefficients c in Table I.

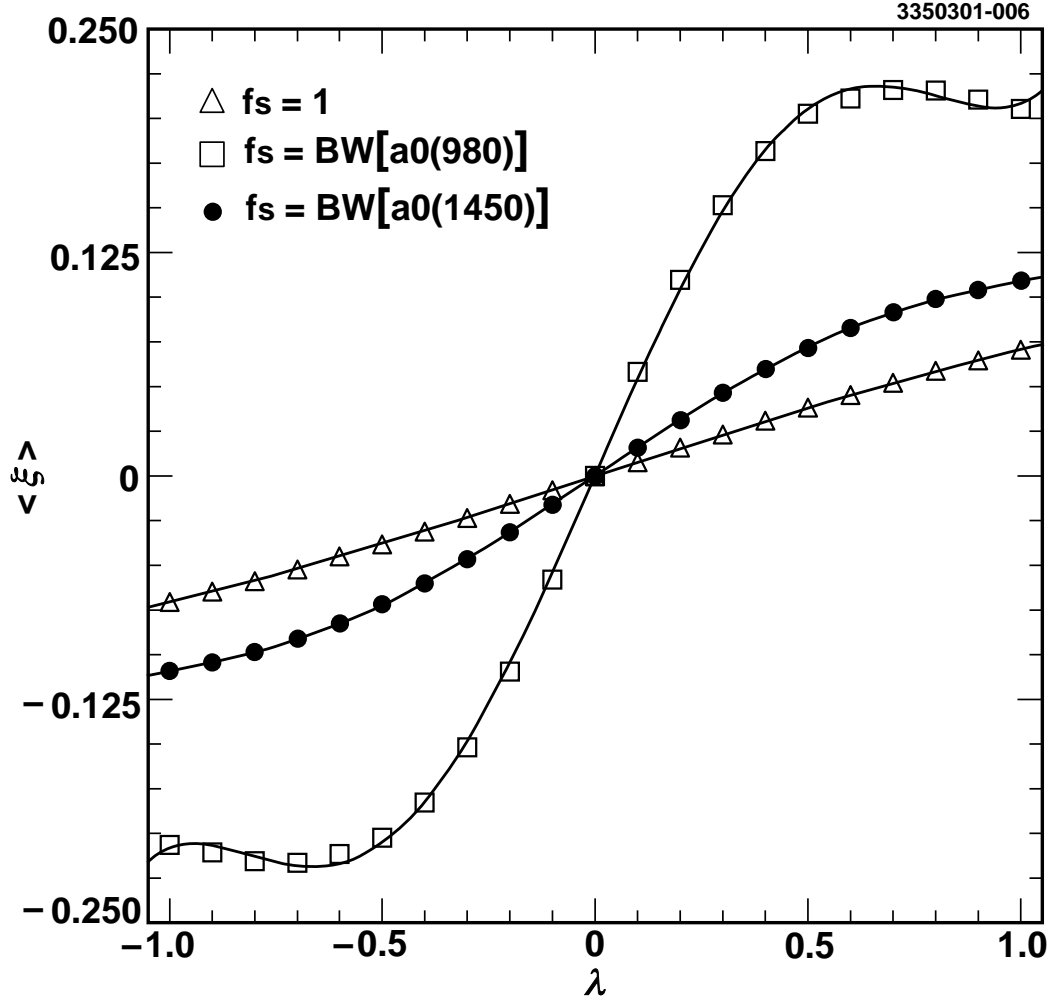


FIG. 6. λ dependence on average value of optimal observable $\langle \xi \rangle$, for different assumptions on scalar form factor f_s .

TABLE I. Average values of the optimal observable $\langle \xi \rangle$ for the Standard Model Monte Carlo and the proportionality coefficient c for the CP asymmetry fits for different scalar form factors.

| Form factor, f_s | $\langle \xi \rangle, 10^{-3}$ | $c, 10^{-3}$ |
|--------------------|--------------------------------|------------------|
| 1 | 0.7 ± 0.6 | 66.8 ± 4.3 |
| $BW(a_0(980))$ | 1.0 ± 1.1 | 586.4 ± 19.4 |
| $BW(a_0(1450))$ | 0.5 ± 0.8 | 145.8 ± 7.3 |

We observe that the event selection criteria do not introduce an artificial asymmetry in the ξ distribution. For all three form factors, the mean value of ξ for the Standard Model Monte Carlo sample is consistent with zero within its statistical error. These fits show no indication that $\langle \xi \rangle$ deviates from linearity within the range determined by event-generator-level Monte Carlo study. We then use the coefficients from Table I to calculate λ .

B. Observed mean values

For each choice of the scalar form factor, we obtain a distribution in ξ , with two entries per event for the two solutions for the tau lepton direction as described in Section III. These distributions are shown in Fig. 7, with those from the Standard Model Monte Carlo simulations overlaid. From these distributions we compute the mean values $\langle \xi \rangle$ after subtracting the average value for Standard Model Monte Carlo, which are reported in the first column of Table II. In each case, we use the appropriate empirically-determined coefficient given in Table I to derive a value for the imaginary part of the Higgs coupling Λ , as described in the preceding section. These values along with the 90% confidence limits on $\Im(\Lambda)$ are reported in the second and third columns of Table II.

TABLE II. Average value of the optimal observable ξ after subtracting the average value for Standard Model Monte Carlo, calculated value of $\Im(\Lambda)$ and 90% C.L. limits on $\Im(\lambda)$.

| Form factor | $\langle \xi \rangle, 10^{-3}$ | $\Im(\Lambda), 10^{-2}$ | $\Im(\Lambda), 90\% \text{ confidence limits}$ |
|-----------------------|--------------------------------|-------------------------|--|
| $f_s = 1$ | -0.8 ± 1.4 | -1.2 ± 2.1 | $-0.046 < \lambda < 0.022$ |
| $f_s = BW(a_0(980))$ | -0.6 ± 2.4 | -0.1 ± 0.4 | $-0.008 < \lambda < 0.006$ |
| $f_s = BW(a_0(1450))$ | 0.2 ± 1.7 | 0.1 ± 1.2 | $-0.019 < \lambda < 0.021$ |

C. Systematic errors

In principle, several possible sources of systematic error can contribute to this analysis. We found no sizable effect to alter the limits shown in Table II. We describe most significant effects below.

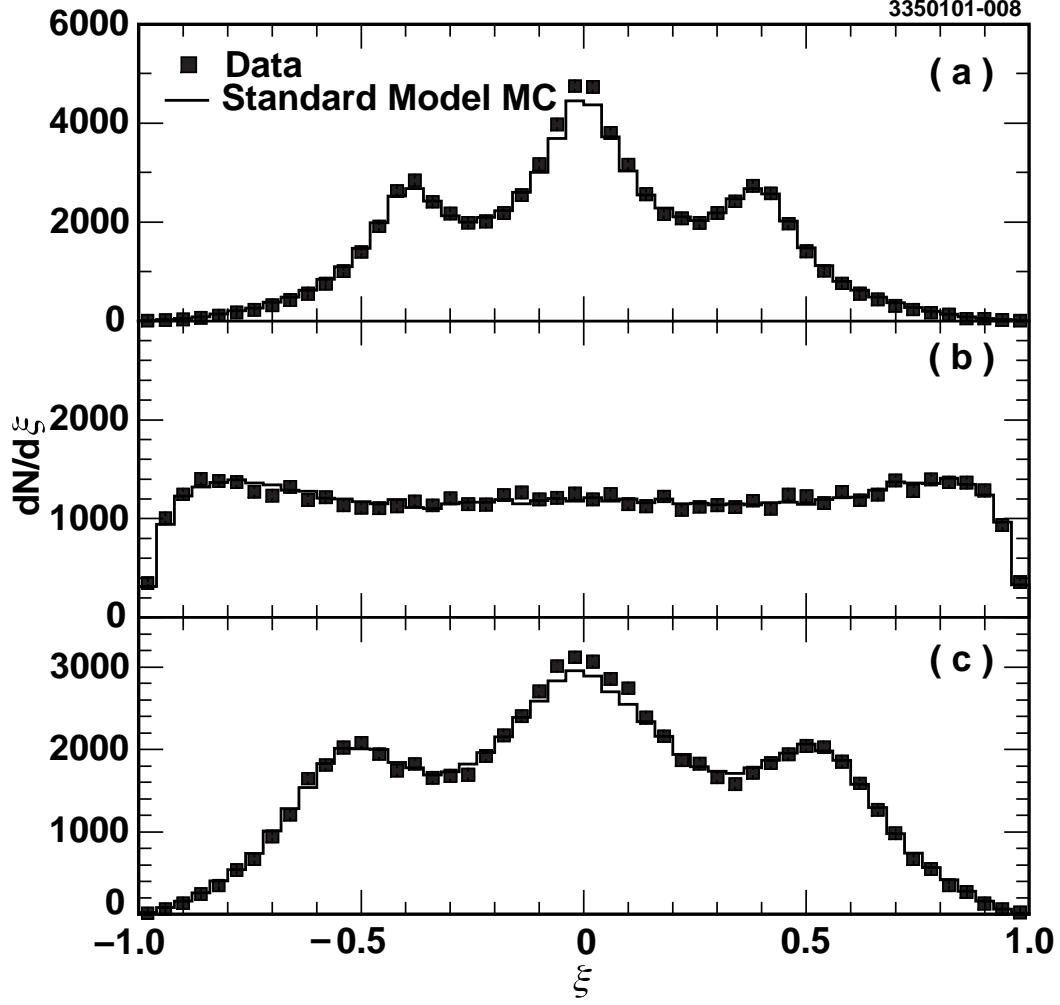


FIG. 7. The distribution of CP violation sensitive variable ξ for the data (dots) compared to the Standard Model Monte Carlo prediction (solid line) for (a) $f_s=1$, (b) $f_s = BW(a_0(980))$ and (c) $f_s = BW(a_0(1450))$.

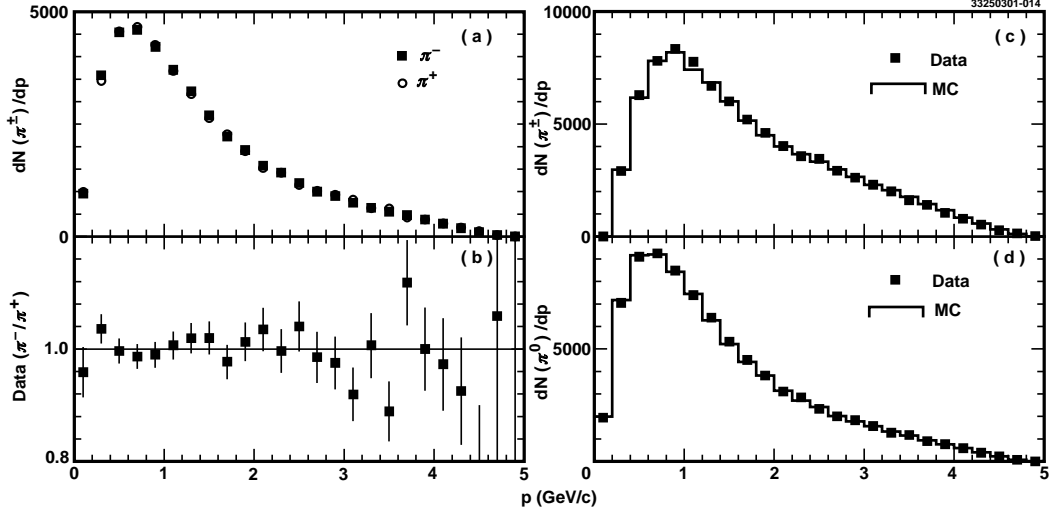


FIG. 8. Momentum distributions for (a) π^- and π^+ in data, (b) π^-/π^+ ratio in data, (c) charged pions, (d) neutral pions.

1. Detector asymmetry

The detector can create an artificial CP asymmetry due to the imperfect tracking, detection efficiency, and resolution. To check the symmetry of the CLEO detector tracking, an independent analysis was done using leptonic tau decays. Such decays have been studied with $\sim 0.1\%$ precision [35] and at that level show no deviation from the Standard Model. Therefore, any observed asymmetry would indicate detector effects. We find the detector response symmetric with respect to the charge within a precision of 0.2% and the detector asymmetry, A , in momentum distribution is:

$$-0.4\% < A < 0.2\% \text{ at } 90\% \text{ C.L.}$$

2. Track reconstruction efficiency

We study the systematic effects due to a possible difference of the track reconstruction efficiency for π^- and π^+ as a function of the pion momentum. To estimate the size of this effect we plot in Fig. 8(a) the momentum distribution for charged pions in the reaction $\tau^\pm \rightarrow \pi^\pm \pi^0 \nu_\tau$. The ratio of these distributions shown in Fig. 8(b) is consistent with 1. The introduction of a $\pm 1\sigma$ slope to the ratio plotted in Fig. 8(b) does not change the value of the coefficient c but changes the value of $\Im(\Lambda)$ by ± 0.003 . We take this as a measure of a systematic error.

3. Momentum reconstruction

Another possible source of systematic error is due to an imperfect Monte Carlo simulation of the momentum distributions for the tau decay products. Monte Carlo describes the data very well [see Fig. 8(c) and Fig. 8(d)]. We estimate the size of the systematic error by introducing artificial

$\pm 1\sigma$ shifts in the slopes of the charged and neutral pions momentum distributions. These shifts do not bias the $\langle \xi \rangle$ measurement, but change the calibration coefficient c . The systematic error on c is estimated to be 2.2×10^{-3} and has a negligible effect ($\sim 10^{-5}$) on the value of $\Im(\Lambda)$.

4. Background

Another source of possible distortion of the result is an asymmetry of the ξ distribution induced by the remaining background. In order to estimate this effect we denote by ξ_S and ξ_B the values of ξ from the signal and background events, respectively. If we denote the number of signal and background events by S and B , then, the observed average value of ξ is:

$$\langle \xi \rangle = \frac{\sum \xi_S + \sum \xi_B}{S + B} = \frac{\sum \xi_S}{S} \times \frac{S}{S + B} + \frac{\sum \xi_B}{B} \times \frac{B}{S + B}. \quad (25)$$

Since the number of background events in this analysis is much smaller than the number of signal events, then this equation can be simplified:

$$\langle \xi \rangle \sim \frac{\sum \xi_S}{S + B} + \frac{\sum \xi_B}{B} \times \frac{B}{S} = \langle \xi_S \rangle + \langle \xi_B \rangle \times \frac{B}{S}, \quad (26)$$

where $\langle \xi_S \rangle$ is a mean value due to signal and $\langle \xi_B \rangle$ is a mean value due to background. We estimate $\langle \xi_B \rangle B/S$ using Monte Carlo:

$$\langle \xi_B \rangle \times \frac{B}{S} = (0.04 \pm 0.04) \times 10^{-3}.$$

Thus, the systematic uncertainty arising from this source is negligible on the scale of the sensitivity of our measurement.

D. Summary

Within our experimental precision we observe no significant asymmetry of the optimal variable and, therefore, no CP violation in τ decays. Due to the uncertainty in the choice of the scalar form factor we select the most conservative 90% confidence limits corresponding to $f_s = 1$:

$$-0.046 < \lambda < 0.022, \text{ at } 90\% \text{ C.L..}$$

These limits include the effects of possible systematic errors.

VI. SEARCH FOR SCALAR-MEDIATED τ DECAYS

The helicity angle, $\theta_{\pi\pi}$, is defined as the angle between the direction of the charged pion in the $\pi\pi^0$ rest frame and the direction of the $\pi\pi^0$ system in the τ rest frame. In Standard Model, the helicity angle is expected to have a distribution corresponding to a vector exchange:

$$\frac{dN}{d \cos \theta_{\pi\pi}} \sim a + b \cos^2 \theta_{\pi\pi}. \quad (27)$$

For scalar-mediated decays, there is an additional term proportional to $\cos \theta_{\pi\pi}$ that corresponds to the S-P wave interference and linearly proportional to the scalar coupling constant Λ . In general,

Λ is complex and the term linear in $\cos \theta_{\pi\pi}$ is proportional to the real and imaginary parts of the scalar coupling with coefficients c_1 and c_2 , respectively:

$$\frac{dN}{d \cos \theta_{\pi\pi}} \sim a + c_1 \Re(\Lambda) \cos \theta_{\pi\pi} + c_2 \Im(\Lambda) \cos \theta_{\pi\pi} + b \cos^2 \theta_{\pi\pi}. \quad (28)$$

The observation of the terms proportional to cosine of the helicity angle would indicate the scalar exchange in the tau decays. In the following, we discuss a model independent method used to extract confidence limits on the imaginary part of the scalar coupling Λ .

In order to calculate the helicity angle we must know the tau rest frame. Due to the unobserved neutrino, the tau rest frame can only be reconstructed with a two-fold ambiguity. We can avoid such ambiguity by using the pseudo-helicity angle, θ^* . This pseudo-helicity angle is obtained by replacing the tau rest frame with the laboratory rest frame where it is defined as an angle between the direction of π^\pm in the $\pi\pi^0$ rest frame and the direction of the $\pi\pi^0$ system in the lab frame. The difference between the pseudo-helicity distributions for the τ^+ and τ^- decays is expected to have the same form as given by Eq. 28 but with a different numerical coefficients.

The term including $\Im(\Lambda)$ changes sign for tau leptons of opposite charges. Therefore, the difference of the pseudo-helicity distributions for positive and negative tau leptons has the term linear in $\cos \theta^*$ proportional to the imaginary part of the scalar coupling Λ only:

$$\frac{dN(\tau^-)}{d \cos \theta^*} - \frac{dN(\tau^+)}{d \cos \theta^*} \sim 2c_2 \Im(\Lambda) \cos \theta^*. \quad (29)$$

The presence of this term indicates CP violation.

In this study, we use the same data sample as for the previous analysis with the same selection criteria except for the requirement of the successful cone reconstruction. The pseudo-helicity distribution for τ^- and τ^+ is given in Fig. 9(a).

The structure in Fig. 9(a) is due to the variation in the efficiency as a function of charged pion momentum and π^0 energy. To obtain the product of the imaginary part of the scalar coupling Λ and a linearity coefficient c_2 (see Eq. 29), we fit the difference of the two pseudo-helicity distributions for negative and positive tau leptons to a first order polynomial. To minimize systematic effects due to soft pion reconstruction we perform the fit in the region of $-0.7 < \cos \theta^* < 0.8$, which corresponds to pions with momentum higher than 0.3 GeV/c. The obtained value of the slope for the data distribution is:

$$c_2 \Im(\Lambda) = (4.2 \pm 3.6) \times 10^{-4}$$

and illustrated in Fig. 9(b). It is consistent with zero within statistical error.

To determine the proportionality coefficient c_2 we follow the procedure described in Section V. We calculate the slope of the difference of pseudo-helicity distributions after applying selection criteria using five samples of 200,000 signal Monte Carlo events generated with different values of λ . Then, we fit the calculated slope dependence as a function of λ using straight line to obtain c_2 :

$$c_2 = (107.5 \pm 12.6) \times 10^{-4}.$$

We use this coefficient to obtain the value of the imaginary part of the scalar coupling $\Im(\Lambda)$:

$$\Im(\Lambda) = 0.028 \pm 0.037, \text{ or } -0.033 < \Im(\Lambda) < 0.089 \text{ at } 90\% \text{ C.L.} \quad (30)$$

As expected, the limit on the $\Im(\Lambda)$ is less strict than the one obtained using the optimal observable.

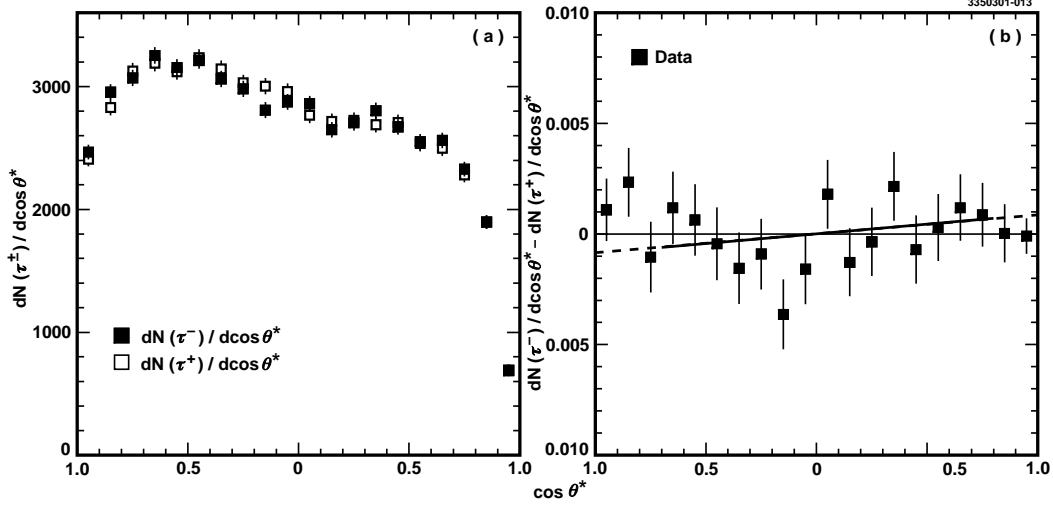


FIG. 9. (a) Pseudo-helicity distribution for τ^- and τ^+ in data, (b) difference between pseudo-helicity distributions for τ^- and τ^+ in data. Solid line is a linear fit and dashed lines show extrapolation to the region excluded from the fit.

VII. CONCLUSIONS

We have discussed a method of searching for the CP violation in the correlated decays of two tau leptons each decaying into the $\pi^\pm\pi^0\nu_\tau$ final state. The limit on the imaginary part of Higgs coupling constant is model dependent and depends on the choice of scalar form factor. The most conservative choice of scalar form factor $f_s = 1$ leads to a conservative limit on a scalar coupling:

$$-0.046 < \Im(\Lambda) < 0.022 \text{ at } 90\% \text{ C.L.}$$

Using pseudo-helicity method we obtain a limit on a imaginary part of the scalar component in the tau decays:

$$-0.033 < \Im(\Lambda) < 0.089 \text{ at } 90\% \text{ C.L.}$$

Both limits agree with each other and restrict the size of the contribution of multi-Higgs doublet model diagrams to the τ lepton decay.

We can relate the limit on $\Im(\Lambda)$ to the limit on the product of multi-Higgs model coupling constants (see Eq. 10):

$$-0.026 \text{ (GeV}/c^2\text{)}^{-1} < \frac{1}{m_{Higgs}^2} (m_u \Im(Z^* Y) - m_d \Im(Z^* X)) < 0.012 \text{ (GeV}/c^2\text{)}^{-1}.$$

VIII. ACKNOWLEDGMENTS

We gratefully acknowledge the effort of the CESR staff in providing us with excellent luminosity and running conditions. M. Selen thanks the PFF program of the NSF and the Research Corporation, and A.H. Mahmood thanks the Texas Advanced Research Program. This work was supported by the National Science Foundation, the U.S. Department of Energy, and the Natural Sciences and Engineering Research Council of Canada.

APPENDIX A: CALCULATION OF THE SQUARED MATRIX ELEMENT FOR THE DECAY $\tau^- \rightarrow \pi^- \pi^0 \nu_\tau$

The matrix elements and their conjugates have the following forms:

$$M(\tau^- \rightarrow \pi^- \pi^0 \nu_\tau) \sim f_V Q^\mu \bar{u}(k) \gamma_\mu (1 - \gamma_5) u(q, s) + \Lambda f_S \bar{u}(k) (1 + \gamma_5) u(q, s), \quad (\text{A1})$$

$$M^*(\tau^- \rightarrow \pi^- \pi^0 \nu_\tau) \sim f_V^* Q^\mu \bar{u}(q, s) \gamma_\mu (1 - \gamma_5) u(k) + \Lambda^* f_S^* \bar{u}(q, s) (1 - \gamma_5) u(k), \quad (\text{A2})$$

$$\bar{M}(\tau^+ \rightarrow \pi^+ \pi^0 \nu_\tau) \sim -f_V Q^\mu \bar{v}(q, s) \gamma_\mu (1 - \gamma_5) v(k) + \Lambda^* f_S \bar{v}(q, s) (1 - \gamma_5) v(k), \quad (\text{A3})$$

$$\bar{M}^*(\tau^+ \rightarrow \pi^+ \pi^0 \nu_\tau) \sim -f_V^* Q^\mu \bar{v}(k) \gamma_\mu (1 - \gamma_5) v(q, s) + \Lambda f_S^* \bar{v}(k) (1 + \gamma_5) v(q, s). \quad (\text{A4})$$

The momentum vectors q , K , Q , and form factors f_v and f_s are defined in section II A. We used the following rules to form complex conjugates: we conjugate all complex numbers, $u \leftrightarrow \bar{u}$, $v \leftrightarrow \bar{v}$, and they exchange places; $1 \leftrightarrow 1$, $\gamma_5 \leftrightarrow -\gamma_5$, $\gamma_\mu \leftrightarrow \gamma_\mu$, $\gamma_\mu \gamma_5 \leftrightarrow \gamma_\mu \gamma_5$. The minus sign at the vector hadronic current of the equations (A3) and (A4) is due to the anti-symmetric behavior of the ρ under the isospin rotation. To form the squared matrix element $|M|^2 = M^* M$, we use:

$$u(\nu) \bar{u}(\nu) = k^\rho \gamma_\rho = v(\nu) \bar{v}(\nu), \quad (\text{A5})$$

$$u(\tau) \bar{u}(\tau) = (q^\alpha \gamma_\alpha + m)(1 + s^\beta \gamma_\beta \gamma_5), \quad (\text{A6})$$

$$v(\tau) \bar{v}(\tau) = (q^\alpha \gamma_\alpha - m)(1 + s^\beta \gamma_\beta \gamma_5). \quad (\text{A7})$$

where s^β is the spin vector(axial) of the tau. Multiplying matrix elements by their complex conjugates gives us the absolute value of the squared matrix element:

$$\begin{aligned} |M|^2 = M^* M \sim & |f_V|^2 Q^\mu Q^\nu (q^\alpha \gamma_\alpha + m)(1 + s^\beta \gamma_\beta \gamma_5) \gamma_\mu (1 - \gamma_5) k^\rho \gamma_\rho \gamma_\nu (1 - \gamma_5) \\ & + |\Lambda|^2 |f_S|^2 (q^\alpha \gamma_\alpha + m)(1 + s^\beta \gamma_\beta \gamma_5) (1 - \gamma_5) k^\rho \gamma_\rho (1 + \gamma_5) \\ & + \Lambda f_S f_V^* Q^\mu (q^\alpha \gamma_\alpha + m)(1 + s^\beta \gamma_\beta \gamma_5) \gamma_\mu (1 - \gamma_5) k^\rho \gamma_\rho (1 + \gamma_5) \\ & + \Lambda^* f_S^* f_V Q^\mu (q^\alpha \gamma_\alpha + m)(1 + s^\beta \gamma_\beta \gamma_5) (1 - \gamma_5) k^\rho \gamma_\rho \gamma_\mu (1 - \gamma_5), \end{aligned} \quad (\text{A8})$$

$$\begin{aligned} |\bar{M}|^2 = \bar{M}^* \bar{M} \sim & |f_V|^2 Q^\mu Q^\nu (q^\alpha \gamma_\alpha - m)(1 + s^\beta \gamma_\beta \gamma_5) \gamma_\mu (1 - \gamma_5) k^\rho \gamma_\rho \gamma_\nu (1 - \gamma_5) \\ & + |\Lambda|^2 |f_S|^2 (q^\alpha \gamma_\alpha - m)(1 + s^\beta \gamma_\beta \gamma_5) (1 - \gamma_5) k^\rho \gamma_\rho (1 + \gamma_5) \\ & - \Lambda^* f_S^* f_V Q^\mu (q^\alpha \gamma_\alpha - m)(1 + s^\beta \gamma_\beta \gamma_5) (1 - \gamma_5) k^\rho \gamma_\rho \gamma_\mu (1 - \gamma_5) \\ & - \Lambda f_S f_V^* Q^\mu (q^\alpha \gamma_\alpha - m)(1 + s^\beta \gamma_\beta \gamma_5) \gamma_\mu (1 - \gamma_5) k^\rho \gamma_\rho (1 + \gamma_5). \end{aligned} \quad (\text{A9})$$

Reducing to the traces, we can write the matrix element squared as follows:

$$\begin{aligned} |M^2| \sim & 2|f_V|^2 (2(q \cdot Q)(k \cdot Q) - (q \cdot k)Q^2) + 2|\Lambda|^2 |f_S|^2 (q \cdot k) + 4\Re(\Lambda f_S f_V^*) m(Q \cdot k) \\ & + 2|f_V|^2 m(2(s \cdot Q)(k \cdot Q) - (s \cdot k)Q^2) - 2|\Lambda|^2 |f_S|^2 m(s \cdot k) \\ & + 4\Re(\Lambda f_S f_V^*) ((s \cdot Q)(q \cdot k) - (s \cdot k)(q \cdot Q)) \\ & + 4\Im(\Lambda f_S f_V^*) \epsilon_{\beta\alpha\mu\rho} s^\beta q^\alpha Q^\mu k^\rho, \end{aligned} \quad (\text{A10})$$

$$\begin{aligned}
|\bar{M}^2| &\sim 2|f_V|^2(2(q \cdot Q)(k \cdot Q) - (q \cdot k)Q^2) + 2|\Lambda|^2|f_S|^2(q \cdot k) \\
&\quad + 4\Re(\Lambda f_S f_V^*)m(Q \cdot k) \\
&\quad - 2|f_V|^2m(2(s \cdot Q)(k \cdot Q) - (s \cdot k)Q^2) + 2|\Lambda|^2|f_S|^2m(s \cdot k) \\
&\quad - 4\Re(\Lambda f_S f_V^*)((s \cdot Q)(q \cdot k) - (s \cdot k)(q \cdot Q)) \\
&\quad + 4\Im(\Lambda f_S f_V^*)\epsilon_{\beta\alpha\mu\rho}s^\beta q^\alpha Q^\mu k^\rho.
\end{aligned} \tag{A11}$$

Combining these two equations, dropping the overall factor of two and using $\Lambda^+ \equiv \Lambda$ for τ^- and $\Lambda^+ \equiv \Lambda^*$ for τ^+ gives us the following expression for the squared matrix element of $\tau^\pm \rightarrow \pi^\pm \pi^0 \nu_\tau$:

$$\begin{aligned}
|M^2| &\sim |f_V|^2(2(q \cdot Q)(k \cdot Q) - (q \cdot k)Q^2) + |\Lambda|^2|f_S|^2(q \cdot k) \\
&\quad + 2\Re(\Lambda^+ f_S f_V^*)m(Q \cdot k) \\
&\quad \pm |f_V|^2m(2(s \cdot Q)(k \cdot Q) - (s \cdot k)Q^2) \mp |\Lambda|^2|f_S|^2m(s \cdot k) \\
&\quad \pm 2\Re(\Lambda^+ f_S f_V^*)((s \cdot Q)(q \cdot k) + (s \cdot k)(q \cdot Q)) \\
&\quad + 2\Im(\Lambda^+ f_S f_V^*)\epsilon_{\beta\alpha\mu\rho}s^\beta q^\alpha Q^\mu k^\rho.
\end{aligned} \tag{A12}$$

We can separate the CP-even and odd part in the squared matrix element by using the following equivalents:

$$\Re(\Lambda^+ f_S f_V^*) = \Re(\Lambda)|f_v||f_s| \cos \delta \mp \Im(\Lambda)|f_v||f_s| \sin \delta, \tag{A13}$$

$$\Im(\Lambda^+ f_S f_V^*) = \Re(\Lambda)|f_v||f_s| \sin \delta \pm \Im(\Lambda)|f_v||f_s| \cos \delta. \tag{A14}$$

Now we can rewrite Eq. A12 as:

$$\begin{aligned}
|\mathcal{M}|_{\tau^\pm \rightarrow \pi^\pm \pi^0 \nu}^2 &\sim |f_v|^2[2(qQ)(kQ) - (kq)Q^2] + |\Lambda|^2|f_s|^2(qk) \\
&\quad 2\Re(\Lambda)|f_v||f_s| \cos \delta M_\tau(Qk) - 2\Im(\Lambda^+)|f_v||f_s| \sin \delta M_\tau(Qk) \\
&\quad + s^\mu \{\pm |f_v|^2 M_\tau(2Q_\mu(kQ) - k_\mu Q^2) \mp |\Lambda|^2|f_s|^2 M_\tau k_\mu \\
&\quad \pm 2\Re(\Lambda)|f_v||f_s| \cos \delta (Q_\mu(kq) - k_\mu(qQ)) \\
&\quad \mp 2\Im(\Lambda^+)|f_v||f_s| \sin \delta (Q_\mu(kq) - k_\mu(qQ)) \\
&\quad + 2\Re(\Lambda)|f_v||f_s| \sin \delta e_{\mu\alpha\beta\gamma} q^\alpha Q^\beta k^\gamma \\
&\quad + 2\Im(\Lambda^+)|f_v||f_s| \cos \delta e_{\mu\alpha\beta\gamma} q^\alpha Q^\beta k^\gamma \}.
\end{aligned} \tag{A15}$$

APPENDIX B: τ -PAIR PRODUCTION AND SPIN CORRELATIONS

The matrix element of $e^+e^- \rightarrow \tau^+\tau^-$ can be written as:

$$M \sim [u(\bar{\tau}^-)\gamma^\mu v(\tau^+)] [\bar{v}(e^+)\gamma_\mu u(e^-)]. \tag{B1}$$

We denote the four-momenta of τ^\pm as q_1 and q_2 , their spins as s_1 and s_2 , respectively, the mass of tau lepton as m and the four-momenta of positron as p_1 and electron as p_2 . We then write the squared matrix element as:

$$|M|^2 \sim Tr(p_1 \gamma_\mu p_2 \gamma_\nu) Tr((1 - \gamma_5 \not{s}_2)(\not{q}_2 + m)\gamma^\mu (1 - \gamma_5 \not{s}_1)(\not{q}_1 - m)\gamma^\nu). \tag{B2}$$

Calculating the traces we get the following expression:

$$\begin{aligned}
|M|^2 \sim & (p_1 \cdot q_1)(p_2 \cdot q_2) + (p_1 \cdot q_2)(p_2 \cdot q_1) + m^2(p_1 \cdot p_2) \\
& - (s_1 \cdot s_2)(p_1 \cdot q_2)(p_2 \cdot q_1) - (s_1 \cdot s_2)(p_1 \cdot q_1)(p_2 \cdot q_2) + (s_1 \cdot s_2)(p_1 \cdot p_2)(q_1 \cdot q_2) \\
& - m^2(s_1 \cdot p_2)(s_2 \cdot p_1) - m^2(s_1 \cdot p_1)(s_2 \cdot p_2) \\
& - (p_1 \cdot p_2)(s_1 \cdot q_2)(s_2 \cdot q_1) - \underline{(p_1 \cdot p_2)(s_1 \cdot q_1)(s_2 \cdot q_2)} \\
& + (p_1 \cdot q_1)(q_2 \cdot s_1)(p_2 \cdot s_2) + (p_1 \cdot q_2)(p_2 \cdot s_1)(q_1 \cdot s_2) \\
& + (p_2 \cdot q_1)(q_2 \cdot s_1)(p_1 \cdot s_2) + (p_2 \cdot q_2)(p_1 \cdot s_1)(q_1 \cdot s_2) \\
& - (q_1 \cdot q_2)(p_2 \cdot s_1)(p_1 \cdot s_2) - (q_1 \cdot q_2)(p_1 \cdot s_1)(p_2 \cdot s_2).
\end{aligned} \tag{B3}$$

The gauge condition $(q_i \cdot s_i) = 0$ leads to a vanishing underlined term. Re-writing the squared matrix element in terms of spin-averaged production P and spin-dependent part $s_{1\mu}s_{2\nu}C^{\mu\nu}$ we obtain the explicit form of the spin-correlation matrix:

$$\begin{aligned}
|M|^2 \sim & P + s_{1\mu}s_{2\nu}C^{\mu\nu} = \\
& (p_1 \cdot q_1)(p_2 \cdot q_2) + (p_1 \cdot q_2)(p_2 \cdot q_1) + m^2(p_1 \cdot p_2) \\
& + s_{1\mu}s_{2\nu}\{-g^{\mu\nu}[(p_1 \cdot q_2)(p_2 \cdot q_1) + (p_1 \cdot q_1)(p_2 \cdot q_2) - (p_1 \cdot p_2)(q_1 \cdot q_2)] \\
& \quad - m^2p_2^\mu p_1^\nu - m^2p_1^\mu p_2^\nu - (p_1 \cdot p_2)q_2^\mu q_1^\nu + (p_1 \cdot q_1)q_2^\mu p_2^\nu \\
& \quad + (p_1 \cdot q_2)p_2^\mu q_1^\nu + (p_2 \cdot q_1)q_2^\mu p_1^\nu + (p_2 \cdot q_2)p_1^\mu q_1^\nu \\
& \quad - (q_1 \cdot q_2)p_2^\mu p_1^\nu - (q_1 \cdot q_2)p_1^\mu p_2^\nu\},
\end{aligned} \tag{B4}$$

or

$$\begin{aligned}
C^{\mu\nu} = & -g^{\mu\nu}[(p_1 \cdot q_2)(p_2 \cdot q_1) + (p_1 \cdot q_1)(p_2 \cdot q_2) - (p_1 \cdot p_2)(q_1 \cdot q_2)] \\
& - m^2p_2^\mu p_1^\nu - m^2p_1^\mu p_2^\nu - (p_1 \cdot p_2)q_2^\mu q_1^\nu + (p_1 \cdot q_1)q_2^\mu p_2^\nu \\
& + (p_1 \cdot q_2)p_2^\mu q_1^\nu + (p_2 \cdot q_1)q_2^\mu p_1^\nu + (p_2 \cdot q_2)p_1^\mu q_1^\nu \\
& - (q_1 \cdot q_2)p_2^\mu p_1^\nu - (q_1 \cdot q_2)p_1^\mu p_2^\nu.
\end{aligned} \tag{B5}$$

The explicit form of the spin-correlation matrix is equal to:

$$\tilde{C}_{\mu\nu} = [g_{\mu\alpha} - \frac{1}{m_\tau^2}q_\mu q_\alpha] C^{\alpha\beta} [g_{\beta\nu} - \frac{1}{m_\tau^2}\bar{q}_\beta \bar{q}_\nu]. \tag{B6}$$

APPENDIX C: CP-EVEN AND ODD PARTS OF TAU PAIR CORRELATED DECAY RATE INTO $(\pi^-\pi^0\nu_\tau) - (\pi^+\pi^0\bar{\nu}_\tau)$

The total probability density for the tau pair decays is given by Eq. 18:

$$P_{\tau^+\tau^-\rightarrow\pi^-\pi^0\nu_\tau\pi^+\pi^0\bar{\nu}_\tau} = G \times \sigma \times \bar{G} + \omega_\mu \tilde{C}^{\mu\nu} \bar{\omega}_\nu, \tag{C1}$$

where G, \bar{G} are the spin-averaged matrix elements squared for τ^-, τ^+ decay (Eq. 15), $\sigma = (p\bar{q})^2 + (\bar{p}q)^2 + m_\tau^2(\bar{p}p)$ is the spin-averaged cross section of $e^+e^- \rightarrow \tau^+\tau^-$, ω^μ and $\bar{\omega}^\nu$ are the polarimeter vectors for τ^- and τ^+ (Eq. 17), and $\tilde{C}_{\mu\nu}$ is the spin-correlation matrix (Eq. B6). Both the spin-averaged matrix element and polarimeter vector of each tau decay contain CP-odd and CP-even

terms. Those terms are contracted with the CP-even tau pair production cross section and spin-correlation matrix. Therefore, the total CP-odd part of Eq. 18 is a product of the CP-even terms of one tau decay contracted with the CP-odd terms of the other tau decay, *i.e.*, it is a linear function of the CP-odd terms. Similarly, the CP-even part of Eq. 18 is equal to the CP-even terms of one tau decay contracted with the CP-even terms of the other tau plus the the CP-odd terms of one tau decay contracted with the CP-odd ones from the other tau decay. This is a sum of the non-CP-violating terms of tau decays and the contraction of the CP-violating terms for both decays simultaneously, where each term remains CP-even. The matrix element for the tau decay is given by Eqs. 15, 16, and 17, where the terms underlined are CP-odd. Thus, the CP-even term of the total cross section is equal to:

$$\begin{aligned}
P_{even} = & \{ |f_v|^2 [2(qQ)(kQ) - (kq)Q^2] + |\Lambda|^2 |f_s|^2 (qk) + 2\Re(\Lambda) |f_v| |f_s| \cos \delta \ M_\tau(Qk) \} \\
& \times \sigma \times \\
& \{ |\bar{f}_v|^2 [2(\bar{q}\bar{Q})(\bar{k}\bar{Q}) - (\bar{k}\bar{q})\bar{Q}^2] + |\Lambda|^2 |\bar{f}_s|^2 (\bar{q}\bar{k}) + 2\Re(\Lambda) |\bar{f}_v| |\bar{f}_s| \cos \bar{\delta} \ M_\tau(\bar{Q}\bar{k}) \} \\
+ & \underline{(-2\Im(\Lambda) |f_v| |f_s| \sin \delta \ M_\tau(Qk))} \times \sigma \times \underline{(-2\Im(\Lambda^*) |\bar{f}_v| |\bar{f}_s| \sin \bar{\delta} \ M_\tau(\bar{Q}\bar{k}))} \\
+ & \{ |f_v|^2 M_\tau(2Q_\mu(kQ) - k_\mu Q^2) - |\Lambda|^2 |f_s|^2 M_\tau k_\mu \\
& + 2\Re(\Lambda) |f_v| |f_s| \cos \delta \ (Q_\mu(kq) - k_\mu(qQ)) + 2\Re(\Lambda) |f_v| |f_s| \sin \delta \ e_{\mu\alpha\beta\gamma} q^\alpha Q^\beta k^\gamma \} \\
& \cdot \tilde{C}^{\mu\nu}. \\
& \{ -|\bar{f}_v|^2 M_\tau(2\bar{Q}_\mu(\bar{k}\bar{Q}) - \bar{k}_\mu \bar{Q}^2) + |\Lambda|^2 |\bar{f}_s|^2 M_\tau \bar{k}_\mu \\
& - 2\Re(\Lambda) |\bar{f}_v| |\bar{f}_s| \cos \bar{\delta} \ (\bar{Q}_\mu(\bar{k}\bar{q}) - \bar{k}_\mu(\bar{q}\bar{Q})) + 2\Re(\Lambda) |\bar{f}_v| |\bar{f}_s| \sin \bar{\delta} \ e_{\nu\alpha\beta\gamma} \bar{q}^\alpha \bar{Q}^\beta \bar{k}^\gamma \} \\
+ & \underline{\{-2\Im(\Lambda) |f_v| |f_s| \sin \delta \ (Q_\mu(kq) - k_\mu(qQ))\}} + \underline{2\Im(\Lambda) |f_v| |f_s| \cos \delta \ e_{\mu\alpha\beta\gamma} q^\alpha Q^\beta k^\gamma} \\
& \cdot \tilde{C}^{\mu\nu}. \\
& \underline{\{2\Im(\Lambda^*) |\bar{f}_v| |\bar{f}_s| \sin \bar{\delta} \ (\bar{Q}_\mu(\bar{k}\bar{q}) - \bar{k}_\mu(\bar{q}\bar{Q}))\}} + \underline{2\Im(\Lambda^*) |\bar{f}_v| |\bar{f}_s| \cos \bar{\delta} \ e_{\nu\alpha\beta\gamma} \bar{q}^\alpha \bar{Q}^\beta \bar{k}^\gamma}. \tag{C2}
\end{aligned}$$

Similarly, the expression for CP-odd part of the tau pair production decaying into $\pi\pi^0\nu_\tau$ state is:

$$\begin{aligned}
P_{odd} = & \{ |f_v|^2 [2(qQ)(kQ) - (kq)Q^2] + |\Lambda|^2 |f_s|^2 (qk) + 2\Re(\Lambda) |f_v| |f_s| \cos \delta \ M_\tau(Qk) \} \\
& \times \sigma \times \underline{((-2\Im(\Lambda^*) |\bar{f}_v| |\bar{f}_s| \sin \bar{\delta} \ M_\tau(\bar{Q}\bar{k}))} \\
+ & \underline{(-2\Im(\Lambda) |f_v| |f_s| \sin \delta \ M_\tau(Qk))} \times \sigma \times \\
& \{ |\bar{f}_v|^2 [2(\bar{q}\bar{Q})(\bar{k}\bar{Q}) - (\bar{k}\bar{q})\bar{Q}^2] + |\Lambda|^2 |\bar{f}_s|^2 (\bar{q}\bar{k}) + 2\Re(\Lambda) |\bar{f}_v| |\bar{f}_s| \cos \bar{\delta} \ M_\tau(\bar{Q}\bar{k}) \} \\
+ & \{ |f_v|^2 M_\tau(2Q_\mu(kQ) - k_\mu Q^2) - |\Lambda|^2 |f_s|^2 M_\tau k_\mu \\
& + 2\Re(\Lambda) |f_v| |f_s| \cos \delta \ (Q_\mu(kq) - k_\mu(qQ)) + 2\Re(\Lambda) |f_v| |f_s| \sin \delta \ e_{\mu\alpha\beta\gamma} q^\alpha Q^\beta k^\gamma \}
\end{aligned}$$

$$\begin{aligned}
& \cdot \tilde{C}^{\mu\nu}. \\
& \{ \underline{2\Im(\Lambda^*)|\bar{f}_v||\bar{f}_s| \sin \bar{\delta} (\bar{Q}_\mu(\bar{k}\bar{q}) - \bar{k}_\mu(\bar{q}\bar{Q}))} + \underline{2\Im(\Lambda^*)|\bar{f}_v||\bar{f}_s| \cos \bar{\delta} e_{\nu\alpha\beta\gamma}\bar{q}^\alpha\bar{Q}^\beta\bar{k}^\gamma} \} \\
+ & \\
& \{ \underline{-2\Im(\Lambda)|f_v||f_s| \sin \delta (Q_\mu(kq) - k_\mu(qQ))} + \underline{2\Im(\Lambda)|f_v||f_s| \cos \delta e_{\mu\alpha\beta\gamma}q^\alpha Q^\beta k^\gamma} \} \\
& \cdot \tilde{C}^{\mu\nu}. \\
& \{ -|\bar{f}_v|^2 M_\tau(2\bar{Q}_\mu(\bar{k}\bar{Q}) - \bar{k}_\mu\bar{Q}^2) + |\Lambda|^2|\bar{f}_s|^2 M_\tau\bar{k}_\mu \\
& - 2\Re(\Lambda)|\bar{f}_v||\bar{f}_s| \cos \bar{\delta} (\bar{Q}_\mu(\bar{k}\bar{q}) - \bar{k}_\mu(\bar{q}\bar{Q})) + 2\Re(\Lambda)|\bar{f}_v||\bar{f}_s| \sin \bar{\delta} e_{\nu\alpha\beta\gamma}\bar{q}^\alpha\bar{Q}^\beta\bar{k}^\gamma \}. \tag{C3}
\end{aligned}$$

APPENDIX D: THE OPTIMAL OBSERVABLE

There is a freedom of choice of the CP sensitive observable ξ used in our search.³ To maximize the sensitivity of the measurement we need to select ξ with a minimal relative statistical error. For N events, the statistical error on the average value $\langle \xi \rangle$ is given by:

$$\Delta\xi = \sqrt{\frac{\langle \xi^2 \rangle - \langle \xi \rangle^2}{N}}. \tag{D1}$$

If the contribution of the CP-odd term is small (*i.e.*, $\Im(\Lambda)$ is small), the $\langle \xi \rangle^2$ term is proportional to $|\Im(\Lambda)|^2$ (see Eq. 23) and can be neglected. Therefore:

$$\Delta\xi \sim \sqrt{\frac{\langle \xi^2 \rangle}{N}} = \sqrt{\frac{\int \xi^2 P dLips}{N \Gamma}}, \tag{D2}$$

where P is a probability density of the process and Γ is a normalization factor, equal to:

$$\Gamma = \int P dLips. \tag{D3}$$

The sensitivity S of this method to the presence of a non-zero value of $\Im(\Lambda)$ is measured by the number of standard deviations of $\langle \xi \rangle$ with respect to zero:⁴

$$S = \frac{\langle \xi \rangle}{\Delta\xi} = \frac{\int \xi P dLips}{\sqrt{\frac{\langle \xi^2 \rangle - \langle \xi \rangle^2}{N}}}. \tag{D4}$$

We can simplify this expression by separating the CP-odd and CP-even parts of the probability density P (see Eq. 19):

$$P = P_{even} + P_{odd}. \tag{D5}$$

The sensitivity becomes:

³We assume that the observable is CP-odd.

⁴The average of the observable ξ is equal to zero if there is no CP violation.

$$S = \sqrt{N \Gamma R}, \text{ where } R = \frac{(\int \xi P_{odd} dLips)^2}{\int \xi^2 (P_{even} + P_{odd}) dLips}. \quad (D6)$$

We can further simplify R by using the fact that $\xi^2 P_{odd}$ is a CP-odd function:

$$\int \xi^2 P_{odd} dLips = 0, \quad (D7)$$

and

$$R = \frac{(\int \xi P_{odd} dLips)^2}{\int \xi^2 P_{even} dLips}. \quad (D8)$$

The only ξ dependent factor in the expression for the sensitivity is R . In order to find an observable which is most sensitive to the CP-odd term, we need to find a function ξ , for which the value of R is maximal. We use the functional differentiation method. R is in extremum, when its first derivative with respect to ξ is equal to zero:

$$\frac{\delta R}{\delta \xi} = \frac{2P_{odd} \int \xi P_{odd} dLips \int \xi^2 P_{even} dLips - 2\xi P_{even} (\int \xi P_{odd} dLips)^2}{(\int \xi^2 P_{even} dLips)^2} = 0, \quad (D9)$$

or:

$$P_{odd} \int \xi P_{odd} dLips \int \xi^2 P_{even} dLips - \xi P_{even} (\int \xi P_{odd} dLips)^2 = 0. \quad (D10)$$

If $\int \xi P_{odd} dLips = 0$, then the condition above is satisfied, but the sensitivity is equal to zero (see Eq. D6), thus such case is not a proper solution. If $\int \xi P_{odd} dLips \neq 0$, then we can simplify Eq. D10 to obtain:

$$P_{odd} \int \xi^2 P_{even} dLips = \xi P_{even} \int \xi P_{odd} dLips. \quad (D11)$$

One of the possible condition for the extremum of R is:

$$\xi_{ext} = A \frac{P_{odd}}{P_{even}}, \quad (D12)$$

where A is an arbitrary constant. The constant A must be real for the variable ξ to be CP-odd. We can decompose any CP-odd observable ξ into ξ_{ext} and the reminder $\hat{\xi} \equiv \xi - \xi_{ext}$:

$$\xi = A \frac{P_{odd}}{P_{even}} + \hat{\xi}. \quad (D13)$$

Substituting the value of ξ into Eq. D8 gives us the following result:

$$R = \frac{(\int A \frac{P_{odd}^2}{P_{even}} dLips + \int \hat{\xi} P_{odd} dLips)^2}{\int A^2 \frac{P_{odd}^2}{\Omega} dLips + 2A \int P_{odd} \hat{\xi} dLips + \int \hat{\xi}^2 P_{even} dLips}. \quad (D14)$$

We can simplify this equation using that fact that value of R does not depend on a constant A (see Eq. D12). We define A such that:

$$\int P_{odd} \hat{\xi} dLips = 0. \quad (D15)$$

Then, the numerator and one of the terms of the denominator of Eq. D14 vanish. To determine the value of A , we multiply left and right sides of Eq. D12 by P_{odd} and integrate over the phase space:

$$\int \hat{\xi} P_{odd} dLips = A \int \frac{P_{odd}^2}{P_{even}} dLips + \int \hat{\xi} P_{odd} dLips, \quad (D16)$$

$$\int \hat{\xi} P_{odd} dLips = \int \xi P_{odd} dLips - A \int \frac{P_{odd}^2}{P_{even}} dLips = 0, \text{ if :} \quad (D17)$$

$$A = \frac{\int \xi P_{odd} dLips}{\int \frac{P_{odd}^2}{P_{even}} dLips}. \quad (D18)$$

Choosing A in this way, we can simplify R , using the property of Eq. D15:

$$R = \frac{(\int \frac{P_{odd}^2}{P_{even}} dLips)^2}{\int \frac{P_{odd}^2}{P_{even}} dLips + \int \hat{\xi}^2 P_{odd} dLips}. \quad (D19)$$

The numerator $(\int \frac{P_{odd}^2}{P_{even}} dLips)^2$ and the first term of the denominator $\int \frac{P_{odd}^2}{P_{even}} dLips$ are positive and do not depend on $\hat{\xi}$. R has a maximal value when the last term in the denominator is equal to zero. This is possible only when $\hat{\xi}$ is equal to zero. Therefore, the value of R is at maximum for $\xi = A \frac{P_{odd}}{P_{even}}$, and ξ is most sensitive to the CP-odd part of the decay rate. Since the sensitivity does not depend on a value of the constant A , we choose $A = 1$ corresponding to:

$$\xi = \frac{P_{odd}}{P_{even}}. \quad (D20)$$

REFERENCES

- [1] A.D. Sakharov, ZhETF Pis. Red. **5**, 32 (1967); JETP Lett. **5**, 24 (1967).
- [2] J.H. Christenson, J.W. Cronin, V.L. Fitch and R. Turlay, Phys. Rev. Lett. **13**, 138 (1964).
- [3] NA48 Collaboration, V. Fanti *et al.*, Phys. Rev. B **465**, 335 (1999); KTeV Collaboration, A. Alavi-Harati *et al.*, Phys. Rev. Lett **83**, 22 (1999).
- [4] KEK-E246 Collaboration, M. Abe *et al.*, Phys. Rev. Lett. **83**, 4253 (1999).
- [5] S.R. Blatt *et al.*, Phys. Rev. D **27**, 1056 (1983).
- [6] I.I. Bigi and A.I. Sanda, *CP Violation*, (Cambridge University Press 1999).
- [7] B. Aubert *et al.* Phys. Rev. Lett. **86**, 2515 (2001).
- [8] A. Abashian *et al.* Phys. Rev. Lett. **86**, 2509 (2001).
- [9] Kamiokande Collaboration, T. Kajita *et al.*, Nucl. Phys. Proc. Suppl. **77**, 123 (1999).
- [10] M.B. Einhorn, J. Wudka, hep-ph/0007285.
- [11] K. Matsuda, N. Takeda, T. Fukuyama, H. Nishiura, Phys. Rev. D **62** 093001 (2000).
- [12] R. Kitano and Y. Okada, hep-ph/0012040.
- [13] Y. Grossman, Nucl. Phys. **B426**, 355 (1994).
- [14] Y. Grossman, Y. Nir, R. Rattazzi, SLAC-PUB-7379, hep-ph 9701231.
- [15] C.H. Albright, J. Smith, S.H.H. Tye, Phys. Rev. D **21**, 711 (1980).
- [16] Y.S. Tsai, Nucl. Phys. Proc. Suppl. **55C**, 293 (1997).
- [17] J.H. Kuhn, E. Mirkes, Phys. Lett. B **398**, 407 (1997).
- [18] H. Burkhardt *et al.*, Phys. Lett. B **160**, 343, (1985).
- [19] D.M. Kaplan, Phys. Rev. D **57**, 3827 (1998), and references therein.
- [20] CLEO Collaboration, S. Anderson *et al.*, Phys. Rev. Lett. **81**, 3823, (1998).
- [21] BELLE Collaboration, *CP/T tests with τ leptons at Belle*, to be published in the proceedings of 30th International Conference on High-Energy Physics (ICHEP 2000), Osaka, Japan, 27 Jul - 2 Aug 2000.
- [22] S. Weinberg, Phys. Rev. Lett. **37**, 657 (1976).
- [23] Y.S. Tsai, Phys. Rev. D **51**, 3172, (1995).
- [24] We thank A. Weinstein and F. Olness for help in this calculation.
- [25] CLEO Collaboration, S. Anderson *etal.*, Phys. Rev. D **61**, 112002, (2000).
- [26] D. Atwood and A. Soni, Phys. Rev. D **45**, 2405 (1992).
- [27] J. Gunion, B. Grzadkowski, X. He, Phys. Rev. Lett. **77**, 5172 (1996).
- [28] KORALB (v. 2.2)/TAUOLA (v. 2.4): S. Jadach, J.H. Kuhn and Z. Was, Comput. Phys. Commun. **36**, 191 (1985) and *ibid* **64**, 275 (1991), *ibid* **76**, 361 (1993). Implementation of the scalar in $\tau \rightarrow \pi\pi^0\nu_\tau$ decay is done by A. Weinstein and M. Schmidtler and can be obtained directly from them (ajw@caltech.edu).
- [29] CLEO Collaboration, R. Balest *et al.*, Phys. Rev. D **47**, 3671 (1993).
- [30] CLEO Collaboration, Y. Kubota *et al.*, Nucl. Instr. and Meth. **A320**, 66 (1992).
- [31] CLEO Collaboration, T.S. Hill, Nucl. Instr. and Meth. **A418**, 32 (1998).
- [32] R. Brun *et al.*, GEANT 3.15, CERN DD/EE/84-1.
- [33] V.M. Budnev *et al.*, Phys. Rep. **C15**, 181 (1975).
- [34] CLEO Collaboration, M. Artuso *et al.*, Phys. Rev. Lett. **73**, 3762 (1994).
- [35] Particle Data Group, D.E. Groom *et al.*, Eur. Phys. J. **C15**, 320 (2000).